Investigation of the Thermal Behavior of Trielaidin between 10 K and 360 K

J. Cees van Miltenburg* and Paul J. van Ekeren

Faculty of Chemistry, Chemical Thermodynamics Group, Debye Institute, Utrecht University, Padualaan 8, 3584 CH Utrecht, The Netherlands

Francois G. Gandolfo and Eckhard Flöter

Unilever Research & Development, P.O. Box 114, 3130 AC Vlaardingen, The Netherlands

Heat capacities of the α- and the *β*-phase of trielaidin were measured from 10 to 360 K. The enthalpy of fusion of the stable *β*-phase was found to be 177.4 J·g^{-1}, the triple point temperature was 314.83 K, and the calculated purity, assuming eutectic behavior of the main component and the impurity, was 96.66 mol %. The enthalpy of fusion of the metastable α-phase was calculated to be 95.1 J·g^{-1}; the melting temperature was estimated to be 288 K from differential scanning calorimetry experiments. The heat capacity of the liquid phase can be given by a simple linear fit between 320 K and 360 K: c_p(l) = (1.327 + 0.002529*T*/K) J·K^{-1}·g^{-1}. To obtain a thermodynamically consistent set of entropy and enthalpy data for both forms, a zero entropy of 0.037 J·K^{-1}·g^{-1} and a zero enthalpy of 41.48 J·g^{-1} had to be used for the α-phase. The origin of these values is discussed.

Introduction

Triacylglycerols (TAGs) are important compounds in the food industry.[1] Trielaidin or 1,2,3-tri(*trans*-9-octadecenoyl)-glycerol, with a molar mass of 885.4 g·mol^{-1}, denoted EEE, has been used in the past as a constituent of many food products such as margarines and chocolate. Trans fatty acids are now thought to be nutritionally undesirable and thus are being removed from most food products. Nevertheless, EEE remains an interesting TAG as it is an unsaturated TAG that behaves as a saturated TAG. A complete thermal investigation by adiabatic calorimetry and differential scanning calorimetry (DSC) of some of the more common TAGs might help to get more insight into crystallization processes of these compounds, which are often complex. Furthermore, the results may be used to predict the behavior of other compounds of this family. We reported earlier on tripalmitin (PPP),[2] which shows great similarity with EEE. Both compounds can be crystallized in two different crystal forms, the α-form being the metastable form and the stable *β*-form. Many triglycerides also show an intermediate form, mostly called the *β*′-form. We, however, did not observe this form in EEE and PPP. The crystal structure of the *β*-form of EEE was reported by Culot et al.[3] The structures of the α- and the *β*-phase grown under different conditions were recently reported by Dohi et al.[5] Kodali et al.[4] made a DSC study of several triglycerides, including EEE, and reported on X-ray experiments as a function of temperature. Synthesis and physicochemical characterization of mixed diacid triglycerides containing elaidic acid like PEP was reported by Elisabettini et al.[6]

Experimental Section

EEE, with a reported purity of 99 mass %, was purchased from Larodan.[7] About 0.4 g was used in the adiabatic calorimetry experiments. The calorimeter (laboratory indication CAL8) and the measuring procedure have been described before.[8] The calorimeter is a scaled down version of CAL 5, which uses up to 10 mL of sample.[9,10] The smaller sample mass used in CAL8 leads to a slightly higher error margin; from calibration experiments, we estimate the error in heat capacity measurements to be within 0.5% and that in latent heat effects such as melting to be about 0.2%. The measuring procedure consists of alternating stabilization periods and heat input periods. The time length of these periods is adapted to the thermal response of the sample. Below 30 K, they generally are in the order of 100 s; in the melting range, stabilization periods of up to 1 h are often used.

The DSC experiments were performed with a Mettler Toledo DSC 821^e, equipped with an intracooler. A sample of 2.23 mg, encapsulated in an aluminum crucible, was used.

Results and Discussion

DSC Experiments. In the first experiment, the sample was first cooled to 248 K. Then the measurement was performed, in which the sample was first heated to 333 K, successively cooled back to 248 K, and finally reheated to 333 K. The heating and cooling rates were 5 K·min^{-1}. The results are presented in Figure 1. During the first heating, an endothermic melting peak was observed from which for the stable *β*-form the melting point was evaluated as 314 K and the enthalpy of fusion as 154 J·g^{-1}. The cooling curve showed crystallization around 286 K; the enthalpy of crystallization was found to be −80 J·g^{-1}. The curve recorded during reheating showed an endothermic effect immediately followed by an exothermic effect (peak temperatures of 289 K and 290 K, respectively). This is interpreted as melting of the metastable α-phase, followed by recrystallization to the stable *β*-phase. This interpretation is supported by X-ray experiments as a function of

10.1021/je034048e CCC: $25.00
Published on Web 06/18/2003

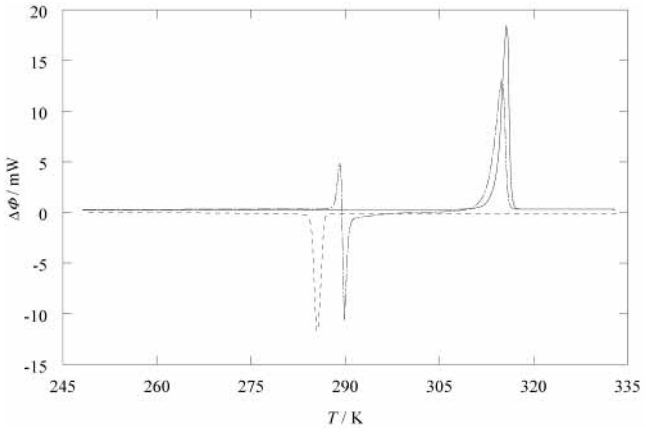

Figure 1. DSC measurement of EEE. The heating curve, at a heating rate of 5 K·min^{-1}, of a fresh sample is given (solid line), together with a cooling curve at a rate of −5 K·min^{-1} (hatched line) and the second heating curve, also at 5 K·min^{-1} (-·-).

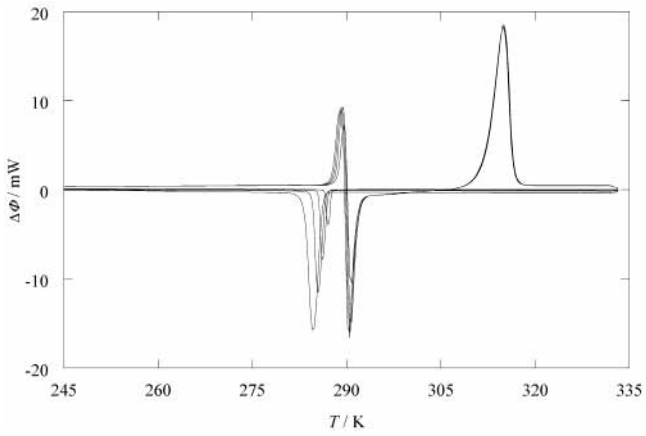

Figure 2. DSC experiments with variable cooling rate, respectively (−1, −2.5, −5, and −10) K·min^{-1}, each followed by a heating curve made at a rate of 10 K·min^{-1}.

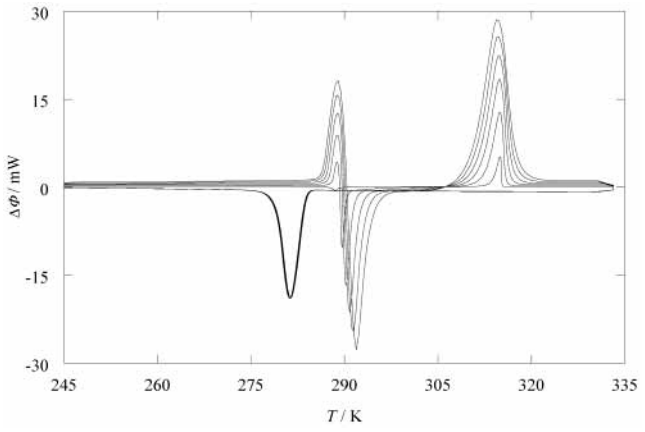

Figure 3. DSC experiments with variable heating rate, respectively (1, 5, 10, 15, 20, and 25) K·min^{-1}. The cooling rate in all cases was −20 K·min^{-1}.

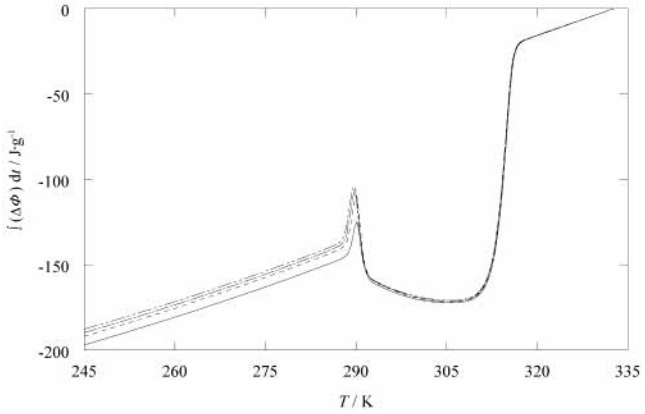

Figure 4. Pseudo-enthalpy calculation of the heating curves in the DSC experiment with variable cooling rate. The curves were matched in the liquid phase. In the low-temperature part, the sequence of the curves follows the sequence of the previous cooling rate; the higher the cooling rate, the higher the pseudo-enthalpy.

temperature.[3,5] From the powder diffraction spectra of Culot et al.,[3] it can be concluded that the α-phase does not contain traces of the *β*-phase. The melting point of the metastable α-phase is estimated as 288 K. At higher temperatures, a second endothermic peak indicated melting of the recrystallized material. The enthalpy of melting for this transition is evaluated as 143 J·g^{-1}; this value is lower than the value found during the first heating, which indicates that the recrystallization from the α-phase to the *β*-phase was not complete.

To investigate the influence of cooling and heating rate, two experiments were performed. In these experiments, cooling and successive heating were repeated several times. In the first experiment, cooling rates of (−1, −2.5, −5, and −10) K·min^{-1} were used, each followed by a heating rate of 10 K·min^{-1}. The results are given in Figure 2. In Figure 3, a cooling rate of −20 K·min^{-1} was used, followed by a variable heating rate of (1, 5, 10, 15, 20, and 25) K·min^{-1}. No phases other than the α- and *β*-phase were observed. After transformation of the heating curves of the experiment with the variable cooling rate, as given in Figure 2, to pseudo-enthalpy curves, it was noticed that the enthalpy of the α-phase depended on the cooling rate. The importance of this observation is discussed further on. The pseudo-enthalpy curves are given in Figure 4.

Adiabatic Calorimetry. From earlier measurements with a slightly less pure sample, we knew that once the compound is melted in the calorimeter, it is very difficult to obtain again the pure *β*-form. This will be discussed further on. So, after loading, the calorimeter was cooled and the measurements were started at 8 K. The set of experimental data up to the liquid phase is given in Table 1. From these measurements, assuming that below 10 K the low-temperature Debye limit for the heat capacity, $C_p = \alpha T^3$, might be used, the entropy and enthalpy values at selected temperatures of the *β*-form were calculated and are given in Table 3. That it was the *β*-form that was measured is very likely, as no exothermic effects were detected during the measurement series. Table 1 consists of data triplets being the mean temperature of the measuring interval, the heat capacity in this interval, and the enthalpy at the mean temperature. In Figure 5, the reciprocal of the melted fraction of the *β*-form is plotted against the equilibrium temperature in the melt. The linear behavior of the curve suggests that impurities form a eutectic system with the main component. The purity calculated, using van't Hoff's law, is 96.66 mol %, and the triple point temperature is (314.83 ± 0.02) K, the enthalpy of fusion being 177.4 J·g^{-1} (or 15.70 kJ·mol^{-1}). In Figure 6, the onset temperatures of crystallization as a function of the cooling rate are given. To obtain the α-phase, crystallization should take place below the melting point of the α-phase. The melting point of the α-form could only be measured with the DSC experiments, which allow higher heating rates. It was found to be (288.0 ± 0.5) K. From Figure 6, it can be seen that a cooling speed of about

Table 1. Experimental Heat Capacity Data and Enthalpy Values of the β-Phase of EEE

T	c_p	$h(T) - h(0)$	T	c_p	$h(T) - h(0)$	T	c_p	$h(T) - h(0)$	T	c_p	$h(T) - h(0)$
K	J·K^{-1}·g^{-1}	J·g^{-1}	K	J·K^{-1}·g^{-1}	J·g^{-1}	K	J·K^{-1}·g^{-1}	J·g^{-1}	K	J·K^{-1}·g^{-1}	J·g^{-1}
10.52	0.004	0.04	104.65	0.739	38.72	206.39	1.195	136.7	288.03	1.743	253.4
11.90	0.010	0.06	107.48	0.753	40.83	208.74	1.206	139.6	290.02	1.762	256.8
12.76	0.027	0.07	110.32	0.765	42.98	211.08	1.217	142.4	292.00	1.785	260.4
14.41	0.033	0.12	113.16	0.779	45.17	213.41	1.228	145.2	293.98	1.809	263.9
16.16	0.050	0.19	116.00	0.792	47.41	215.72	1.240	148.1	295.95	1.832	267.5
17.98	0.067	0.29	118.85	0.806	49.68	218.01	1.252	151.0	297.92	1.860	271.1
19.96	0.085	0.44	121.70	0.819	52.00	220.30	1.262	153.8	299.88	1.886	274.8
22.02	0.106	0.64	124.56	0.829	54.35	222.57	1.273	156.7	301.84	1.930	278.6
24.22	0.126	0.89	127.41	0.839	56.73	224.83	1.285	159.6	303.79	1.968	282.3
26.50	0.147	1.20	130.27	0.857	59.15	227.07	1.298	162.5	305.74	2.028	286.2
28.88	0.169	1.57	133.13	0.866	61.62	229.31	1.311	165.4	307.67	2.135	290.2
32.40	0.259	2.33	135.99	0.876	64.11	231.53	1.321	168.3	309.58	2.393	294.6
35.94	0.243	3.12	138.85	0.888	66.63	233.74	1.333	171.3	311.37	3.495	299.8
38.34	0.288	3.74	141.71	0.899	69.18	235.94	1.345	174.2	312.77	8.572	307.6
40.46	0.302	4.35	144.57	0.909	71.77	238.13	1.357	177.2	313.62	23.79	319.1
42.73	0.299	5.03	147.42	0.921	74.37	240.31	1.369	180.1	314.05	53.27	333.5
45.11	0.328	5.78	150.23	0.934	76.98	242.48	1.381	183.1	314.27	98.76	349.2
47.47	0.352	6.58	153.02	0.946	79.59	244.64	1.395	186.1	314.40	167.14	365.5
49.86	0.372	7.44	155.77	0.960	82.22	246.79	1.407	189.1	314.49	256.18	382.2
52.29	0.393	8.37	158.51	0.973	84.86	248.93	1.419	192.2	314.54	411.18	399.0
54.77	0.415	9.37	161.21	0.984	87.50	251.06	1.433	195.2	314.57	621.70	416.0
57.28	0.440	10.44	163.89	0.998	90.16	253.19	1.445	198.2	314.60	600.53	433.0
59.83	0.462	11.59	166.55	1.009	92.82	255.30	1.460	201.3	314.65	232.84	449.9
62.40	0.463	12.78	169.18	1.022	95.50	257.41	1.474	204.4	314.80	66.64	466.1
65.01	0.492	14.02	171.79	1.033	98.18	259.50	1.491	207.5	315.46	9.347	478.9
67.64	0.517	15.35	174.38	1.047	100.9	261.59	1.505	210.6	317.00	2.145	486.1
70.30	0.535	16.74	176.95	1.058	103.6	263.67	1.520	213.8	318.99	2.131	490.4
72.97	0.553	18.20	179.50	1.070	106.3	265.75	1.537	217.0	321.00	2.141	494.7
75.67	0.569	19.71	182.03	1.082	109.0	267.81	1.552	220.1	323.01	2.142	499.0
78.39	0.589	21.28	184.54	1.096	111.7	269.86	1.569	223.4	325.03	2.149	503.3
81.12	0.605	22.91	187.03	1.105	114.5	271.91	1.585	226.6	327.05	2.153	507.7
83.86	0.622	24.59	189.51	1.117	117.2	273.95	1.603	229.8	329.07	2.159	512.0
86.62	0.639	26.33	191.97	1.128	120.0	275.98	1.624	233.1	331.09	2.164	516.4
89.39	0.656	28.12	194.42	1.139	122.8	278.00	1.643	236.4	333.11	2.167	520.8
92.18	0.672	29.97	196.84	1.152	125.5	280.02	1.662	239.7	335.13	2.171	525.2
95.56	0.688	32.26	199.25	1.162	128.3	282.03	1.682	243.1	337.15	2.176	529.5
99.01	0.711	34.64	201.65	1.172	131.1	284.04	1.705	246.5	339.17	2.184	533.9

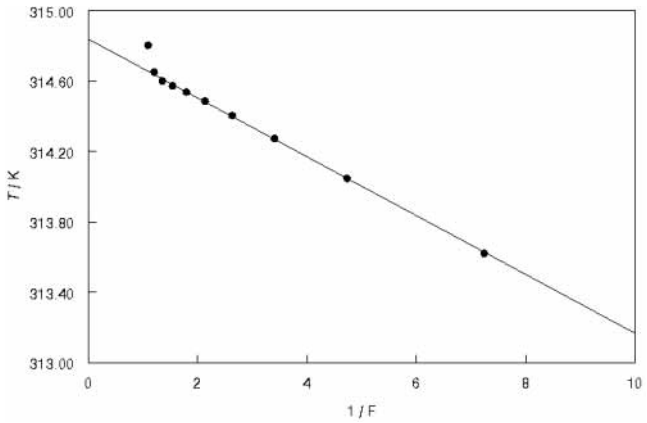

Figure 5. Equilibrium temperatures in the melt against the reciprocal of the melted fraction of the β-phase of EEE.

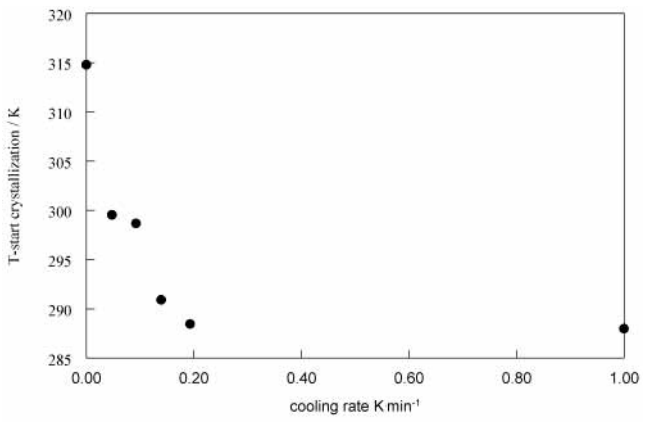

Figure 6. Temperatures at which the crystallization of EEE started as a function of the cooling rate.

0.3 K·min^{-1} or larger is needed to undercool the liquid phase below the melting point of the α-phase. Cooling experiments with lower cooling speeds all resulted in a slow crystallization above the melting point of the α-phase. When the compound was crystallized above the melting temperature of the α-phase, the crystals formed seemed to be imperfect β-form crystals, as during measurement up to the melting point of the β-phase, exothermic effects could be seen in the stabilization periods. The experimental data set of the α-phase is given in Table 2. The heat capacity curves of both phases are given in Figure 7.

Calculation of the entropy and enthalpy data of the α-phase was done in two steps. First, the experimental heat capacity data were used with the assumption that below 10 K the heat capacity data could be represented by $C_p = \alpha T^3$. The enthalpy of the liquid phase of both measurement series was equalized by adding 41.48 J·g^{-1} to the second series. This corresponds to the difference in enthalpy of the α- and β-phase at 0 K and is included in Table 2. Second, the entropy value of the undercooled liquid was calculated at 288 K, using a linear fit of the heat capacity data from the experiments with the β-phase. The fit used was a simple linear function: $c_p(\mathrm{l}) = (1.327 + 0.002529T/\mathrm{K})$ J·K^{-1}·g^{-1}. The difference in enthalpy of the back-extrapolated liquid value and the value of the solid phase of the α-crystals at 288 K is the enthalpy of fusion of the α-phase,

Table 2. Experimental Heat Capacity Data and Enthalpy Values of the α-Phase of EEE

T	c_p	$h(T) - h(0)$	T	c_p	$h(T) - h(0)$	T	c_p	$h(T) - h(0)$	T	c_p	$h(T) - h(0)$
K	J·K^{-1}·g^{-1}	J·g^{-1}	K	J·K^{-1}·g^{-1}	J·g^{-1}	K	J·K^{-1}·g^{-1}	J·g^{-1}	K	J·K^{-1}·g^{-1}	J·g^{-1}
8.85	0.003	41.49	66.67	0.527	56.81	176.16	1.140	149.2	278.01	1.838	309.2
9.73	0.010	41.51	69.33	0.543	58.23	179.08	1.155	152.6	280.48	1.568	313.4
10.55	0.013	41.51	72.01	0.565	59.71	181.99	1.178	156.0	283.23	0.200	315.7
11.43	0.022	41.54	74.71	0.583	61.26	184.90	1.204	159.4	288.45	−3.766	302.0
12.54	0.028	41.55	77.43	0.600	62.87	187.79	1.220	162.9	293.81	−0.377	287.4
13.08	0.032	41.58	80.16	0.619	64.53	190.66	1.247	166.5	296.47	0.133	286.9
14.42	0.041	41.61	82.91	0.636	66.26	193.50	1.271	170.1	298.84	0.887	288.3
14.92	0.046	41.65	85.67	0.656	68.04	196.32	1.296	173.7	301.55	0.947	290.7
16.44	0.057	41.71	88.45	0.672	69.88	199.11	1.321	177.3	304.22	1.063	293.4
16.93	0.064	41.76	91.24	0.689	71.78	201.89	1.346	181.0	306.83	1.276	296.5
18.55	0.080	41.85	94.03	0.706	73.73	204.65	1.371	184.8	309.32	1.858	300.4
18.95	0.085	41.91	96.84	0.722	75.73	207.38	1.398	188.6	311.51	3.658	306.2
20.71	0.101	42.05	99.66	0.739	77.79	210.10	1.423	192.4	313.04	11.98	316.3
21.09	0.106	42.11	100.50	0.742	78.41	212.79	1.446	196.3	313.82	35.54	331.4
22.99	0.125	42.30	103.85	0.766	80.90	215.47	1.472	200.2	314.18	79.81	349.2
23.34	0.128	42.37	106.65	0.779	83.06	218.13	1.494	204.1	314.36	145.03	368.2
25.34	0.147	42.62	109.51	0.792	85.31	220.78	1.517	208.1	314.47	239.73	387.7
25.67	0.152	42.70	112.39	0.807	87.60	223.41	1.539	212.1	314.54	381.31	407.5
27.78	0.168	43.00	115.27	0.821	89.94	226.02	1.564	216.2	314.59	479.55	427.4
28.07	0.170	43.08	118.14	0.836	92.33	228.62	1.587	220.3	314.64	314.19	447.2
30.29	0.190	43.45	121.03	0.851	94.76	231.20	1.608	224.4	314.78	86.83	466.5
30.55	0.194	43.53	123.91	0.865	97.23	233.77	1.630	228.5	315.72	5.549	480.5
31.33	0.208	43.69	126.79	0.879	99.74	236.32	1.653	232.7	317.71	2.128	487.6
31.83	0.222	43.79	129.68	0.895	102.3	238.87	1.676	237.0	320.03	2.136	492.5
33.13	0.223	44.07	132.57	0.910	104.9	241.40	1.698	241.2	322.34	2.139	497.5
33.17	0.221	44.12	135.47	0.918	107.6	243.91	1.721	245.5	324.66	2.148	502.5
35.40	0.248	44.63	138.36	0.934	110.2	246.41	1.745	249.9	326.98	2.154	507.4
37.51	0.267	45.17	141.26	0.952	113.0	248.90	1.768	254.2	329.29	2.161	512.4
39.64	0.287	45.76	144.16	0.960	115.8	251.38	1.792	258.6	331.61	2.167	517.5
41.87	0.308	46.42	147.07	0.976	118.6	253.84	1.816	263.1	333.92	2.171	522.5
44.15	0.330	47.15	149.97	0.989	121.4	256.30	1.840	267.6	336.24	2.176	527.5
46.49	0.353	47.94	152.88	1.002	124.3	258.74	1.867	272.1	338.55	2.183	532.5
48.88	0.376	48.81	155.78	1.024	127.2	261.18	1.892	276.7	340.87	2.192	537.6
51.31	0.396	49.75	158.69	1.036	130.2	263.60	1.917	281.3	343.19	2.198	542.7
53.78	0.418	50.76	161.60	1.053	133.3	266.01	1.940	285.9	345.51	2.203	547.8
56.30	0.444	51.84	164.51	1.069	136.4	268.41	1.957	290.6	347.83	2.207	552.9
58.84	0.466	52.99	167.42	1.087	139.5	270.81	1.968	295.3	350.15	2.217	558.0
61.42	0.481	54.21	170.34	1.104	142.7	273.20	1.963	300.0			

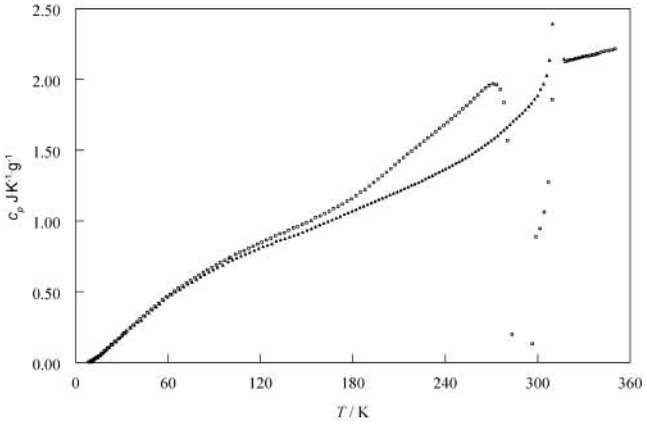

Figure 7. Experimental heat capacities of the two forms of EEE. The β-phase is given by the symbol ▲, the α-phase by □. Recrystallization of the α-phase starts around 278 K.

being 95.1 J·g^{-1}. Then it was possible to calculate the entropy of the α-phase at the melting point, being the entropy of the liquid at 288 K minus the enthalpy of fusion of the α-phase divided by the melting temperature. A zero entropy of 0.037 J·K^{-1}·g^{-1}, or 32.7 J·K^{-1}·mol^{-1}, had to be added to the entropy values calculated directly from the heat capacity measurements of the α-phase to obtain the same value for the liquid phase at the melting point. The entropy and enthalpy values at selected temperatures are given for the β- and the α-phase in Table 3. Values obtained by extrapolation are given in italics. The zero entropy of 32.7 J·K^{-1}·mol^{-1} is large compared to the value reported for PPP. For that compound, a zero entropy of 18 J·K^{-1}·mol^{-1} was reported, and as a possible explanation random freezing-in of rotational positions of the fatty acid chains was suggested. Our DSC experiments, however, do indicate another explanation. Experiments with different cooling rates in the DSC strongly suggest that the α-phase can have different enthalpy values depending on the cooling rate. The higher the cooling rate, the higher the enthalpy value of the α-phase. In Figure 4, the pseudo-enthalpy values calculated from the set of DSC experiments, in which different cooling rates were used but in which all heating experiments were made using a heating rate of 5 K·min^{-1} as given in Figure 2, are given. The pseudo-enthalpy values are calculated by integrating the measured heat-flow signal over time; this implies that the results are not corrected for the difference in mass between the sample and reference pan and for the imbalance of the DSC. The differences in enthalpy can be due to imperfect crystallization or to the occurrence of noncrystalline parts in the sample. We did check all adiabatic calorimetry measurements on the α-phase to see if there was an indication of a glass transition. The telltale behavior of the temperature drift in the stabilization periods (a positive drift when the glass transition is approached, followed by a negative drift when the enthalpy is recovered) was not found. This, however, does not exclude the possibility that a part of the α-phase is amorphous as the glass transition of a small part of the sample will be very weak. In Figure 8, the entropy curves of the two phases are given together

Table 3. Heat Capacities, Entropy, Enthalpy, and Gibbs Energy Values for the β- and α-Phase of EEE at Selected Temperatures

	β-phase				α-phase				liquid
T/K	c_p/J·K^{-1}·g^{-1}	s/J·K^{-1}·g^{-1}	$h - h(0)$/J·g^{-1}	g/J·K^{-1}·g^{-1}	c_p/J·K^{-1}·g^{-1}	s/J·K^{-1}·g^{-1}	$h - h(0)$/J·g^{-1}	g/J·K^{-1}·g^{-1}	s/J·K^{-1}·g^{-1}
20	0.09	0.03	0.44	−0.2	0.10	0.07	42.0	40.6	
25	0.13	0.05	0.99	−0.4	0.14	0.10	42.6	40.1	
30	0.19	0.08	1.77	−0.7	0.19	0.13	43.4	39.6	
35	0.23	0.11	2.82	−1.2	0.24	0.16	44.5	38.8	
40	0.28	0.15	4.13	−1.8	0.29	0.20	45.9	37.9	
45	0.33	0.19	5.66	−2.7	0.34	0.24	47.4	36.9	
50	0.37	0.22	7.41	−3.7	0.39	0.27	49.2	35.6	
55	0.42	0.26	9.38	−4.9	0.43	0.31	51.3	34.1	
60	0.46	0.30	11.6	−6.3	0.47	0.35	53.5	32.5	
65	0.50	0.34	13.9	−7.9	0.51	0.39	56.0	30.6	
70	0.53	0.37	16.5	−9.6	0.55	0.43	58.6	28.5	
75	0.57	0.41	19.3	−11.6	0.59	0.47	61.4	26.3	
80	0.60	0.45	22.2	−13.8	0.62	0.51	64.4	23.9	
85	0.63	0.49	25.2	−16.1	0.65	0.55	67.6	21.2	*0.18*
90	0.66	0.52	28.4	−18.6	0.68	0.58	70.9	18.4	*0.26*
95	0.69	0.56	31.8	−21.3	0.71	0.62	74.4	15.4	*0.35*
100	0.72	0.60	35.3	−24.2	0.74	0.66	78.0	12.2	*0.42*
105	0.74	0.63	38.9	−27.3	0.77	0.70	81.8	8.8	*0.50*
110	0.76	0.67	42.7	−30.5	0.80	0.73	85.7	5.3	*0.57*
120	0.81	0.73	50.5	−37.5	0.85	0.80	93.9	−2.4	*0.71*
130	0.86	0.80	58.8	−45.2	0.90	0.87	102.6	−10.8	*0.84*
140	0.89	0.87	67.6	−53.5	0.94	0.94	111.8	−19.9	*0.96*
150	0.93	0.93	76.7	−62.5	0.99	1.01	121.5	−29.6	*1.08*
160	0.98	0.99	86.2	−72.0	1.04	1.07	131.6	−39.9	*1.19*
170	1.03	1.05	96.3	−82.3	1.10	1.14	142.3	−51.0	*1.29*
180	1.07	1.11	106.7	−93.1	1.16	1.20	153.7	−62.7	*1.39*
190	1.12	1.17	117.7	−104.4	1.24	1.27	165.7	−75.1	*1.49*
200	1.17	1.23	129.1	−116.5	1.33	1.33	178.5	−88.1	*1.58*
210	1.21	1.29	141.0	−129.1	1.42	1.40	192.3	−101.8	*1.67*
220	1.26	1.34	153.4	−142.1	1.51	1.47	206.9	−116.1	*1.76*
230	1.31	1.40	166.2	−155.8	1.60	1.54	222.5	−131.1	*1.84*
240	1.37	1.46	179.6	−170.1	1.69	1.61	238.9	−146.8	*1.92*
250	1.43	1.51	193.6	−184.9	1.78	1.68	256.2	−163.3	*2.00*
260	1.49	1.57	208.2	−200.3	1.88	1.75	274.5	−180.3	*2.08*
270	1.57	1.63	223.5	−216.4	1.97	1.82	293.6	−198.2	*2.15*
280	1.66	1.69	239.6	−233.0	2.05	1.89	313.7	−216.7	*2.23*
288	1.75	1.73	253.3	−246.5	2.13	1.95	330.4	−232.1	*2.28*
288	1.75	1.73	253.3	−246.5	2.05	*2.28*	*425.5*	−232.1	*2.28*
290	1.76	1.75	256.7	−250.2	2.06	*2.30*	*429.6*	−236.7	*2.30*
298.15	1.86	1.80	271.5	−264.6	2.08	*2.36*	*446.5*	−255.7	*2.36*
300	1.89	1.81	274.9	−267.9	2.08	*2.37*	*450.3*	−260.0	*2.37*
310	1.99	1.87	294.3	−286.3	2.11	*2.44*	*471.3*	−284.1	*2.44*
314.83	2.04	1.89	304.1	−295.4	2.12	*2.47*	*481.5*	−295.9	*2.47*
314.83	2.12	2.49	482.5	−295.4	2.12	*2.49*	*487.0*	−295.4	*2.47*
320	2.14	2.50	492.5	−308.5	2.14	*2.50*	*492.5*	−308.5	2.50
330	2.16	2.57	514.0	−334.1	2.16	*2.57*	*514.0*	−334.1	2.57

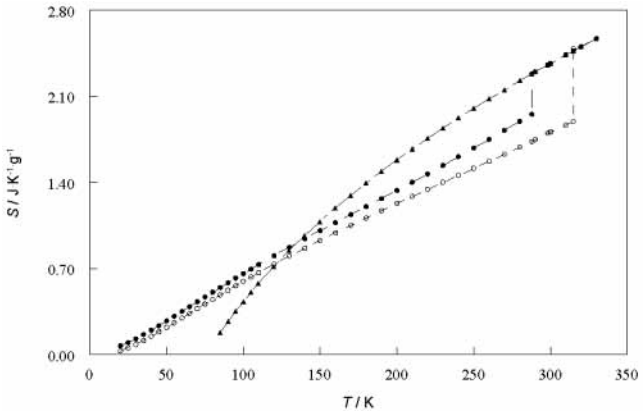

Figure 8. Entropy against temperature curves for the β-phase (○), the α-phase (●), and the liquid phase (▲). The extrapolated values for the liquid phase were calculated using a linear function for the heat capacity above the melting point of the β-phase.

with the back-extrapolated entropy of the liquid phase. If EEE can form a glass, then the glass temperature should be found above the crossing point of the entropy of the solid and the liquid, the so-called Kauzmann temperature. For the β-phase, a Kauzmann temperature of 138 K was found, and for the α-phase, 123 K. Figure 9 gives the enthalpy curves around the melting point of the α-phase. No endothermic melting effect could be observed; the liquid phase seems to be transformed directly to the β-phase. The transition is very slow. In Figure 9, two series of measurements on the α-phase are given. The series represented by the closed triangles was measured with stabilization times of 1200 s and 300 s input time, and the series given by the closed dots, with both times at 300 s. Both series do not reach the enthalpy value of the stable β-phase till the temperature is about 310 K. In another experiment, the α-phase was stabilized at 288 K and left under adiabatic conditions. The temperature of the vessel increased spontaneously, however not to the value expected from the enthalpy curves of the vessel and its contents. After leaving the sample at 290 K for 4 weeks, the measurement was resumed up to the liquid phase. From the exothermic behavior in the stabilization periods before the melting point, it was clear that the sample had not transformed completely to the β-phase. So it seems that to prepare a stable sample, completely in the β-phase, from a once-

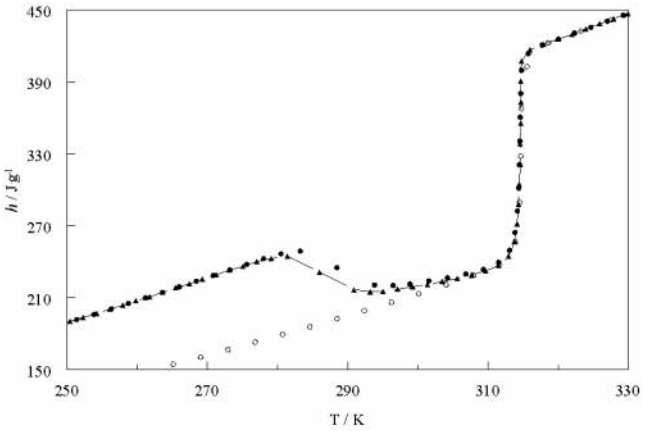

Figure 9. Experimental enthalpy values around the α−β transition and the melting point of the β-phase. The values for the β-phase are given by the symbol ○. For the α-phase, two series are given: ●, measured with stabilization times of 300 s; -▲-, with stabilization times of 1200 s.

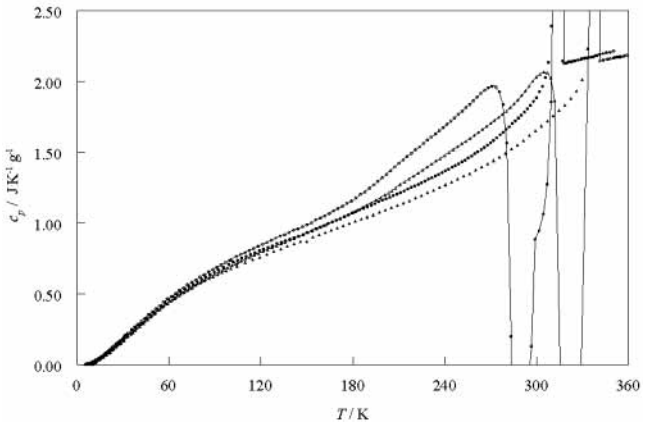

Figure 10. Comparing the heat capacities of EEE and PPP. The values for EEE are given by the symbols ● for the β-phase and -○- for the α-phase; for PPP, the symbols ▲ for the β-phase and -△- for the α-phase are used.

melted compound, stabilization close to the melting point, but at least at 310 K, is needed.

Discussion

The thermodynamic properties of the β-phase of EEE were measured from 5 K to 360 K. The measured heat capacities and the derived properties are probably accurate to within 1%. The measurements of the same properties of the α-phase were complicated by the dependence of the enthalpy on the cooling rate. To obtain a consistent set of thermodynamic data for both polymorphic forms of EEE, a zero entropy of 32.7 $J \cdot K^{-1} \cdot mol^{-1}$ is needed for the α-phase. If different cooling conditions had been chosen, this value would probably be different. One might question if this zero entropy is to be attributed to a form of frozen-in disorder in the α-crystals or to an incomplete crystallization of the α-phase leading to a situation where a part of sample is in the glass phase. Dohi et al.[5] reported that the disorder in the α-phase depended on the crystallization conditions and attributed this to the high undercooling needed to form the α-phase and the difficulty for the methyl side chains to rearrange their position as this involves a displacement of an extensive surrounding area. As we could not find a glass transition, we assume that the disorder in the arrangement of the methyl side chains is the cause of the zero entropy.

A second complication is the recrystallization of the β-phase from the α-phase. When the α-phase was heated, the first exothermic effects, indicating a recrystallization, started at around 278 K. The recrystallization speed reached a maximum at 289 K and continued at a much lower speed to about 314 K. It seems that when the measurements are interrupted between 289 K and 314 K, the recrystallization stops and the degree of metastability in the sample remains almost the same for a long period of time. The great similarity of the thermal properties of EEE and PPP is illustrated in Figure 10, in which the heat capacities of the α- and β-phase of both compounds are given.

Literature Cited

(1) Small, D. M. General Phase Behaviour of Triglycerides. In *Handbook of Lipid Research*: *4. The Physical Chemistry of Lipids*; Plenum Press: New York, 1986.
(2) van Miltenburg, J. C.; ten Grotenhuis, E. A Thermodynamic Investigation of Tripalmitin. Molar Heat Capacities of the α- and β-form between 10 K and 350 K. *J. Chem. Eng. Data* **1999**, *44*, 721−726.
(3) Culot, C.; Norberg, B.; Evrard, G.; Durant, F. Molecular Analysis of the β-polymorphic Form of Trielaidin: Crystal Structure at Low Temperature. *Acta Cryst.* **2000**, *B56*, 317−321.
(4) Kodali, D. R.; Atkinson, D.; Redgrave, T. G.; Small, D. M. Structure and Polymorphism of 18-Carbon Fatty Acyl Triacylglycerols: Effect of Unsaturation and Substitution in the 2-Position. *J. Lipid Res.* **1987**, *28*, 403−413.
(5) Dohi, K.; Kaneko, F.; Kawaguchi, T. X-Ray and Vibrational Spectroscopy Study on Polymorphism of Trielaidin. *J. Cryst. Growth* **2002**, *237−239*, 2227−2232.
(6) Elisabettini, P.; Lognay, G.; Desmedt, A.; Culot, C.; Istasse, N.; Deffense, E.; Durant, F. Synthesis and Physicochemical Characterisation of Mixed Diacid Triglycerides That Contain Elaidic Acid. *J. Am. Oil Chem. Soc.* **1998**, *75*, 285−291.
(7) Larodan−the Lipid and Research Chemicals Company. Web-address: http://www.larodan.se.
(8) van Miltenburg, J. C.; van den Berg, G. J. K.; van Genderen, A. C. G. An Adiabatic Calorimeter for Small Samples. The Solid−Liquid System Naphthalene−Durene. *Thermochim. Acta* **2002**, *383*, 13−19.
(9) van Miltenburg, J. C.; Berg, G. J. K. van den; van Bommel, M. J. Construction of an Adiabatic Calorimeter. Measurement of the Molar Heat Capacity of Synthetic Sapphire and of *n*-Heptane. *J. Chem. Thermodyn.* **1987**, *19*, 1129−1137.
(10) van Miltenburg, J. C.; van Genderen, A. C. G.; van den Berg, G. J. K. Design Improvements in Adiabatic Calorimetry. The Heat Capacity of Cholesterol Between 10 and 425 K. *Thermochim. Acta* **1998**, *319*, 151−162.

Received for review March 4, 2003. Accepted May 21, 2003.

JE034048E